

Interface engineering of domain structures in BiFeO₃ thin films

Deyang Chen, Zuhuang Chen, Qian He, Claudy R. Serrao, James D. Clarkson, Ajay Yadav, Mark E. Nowakowski, Xingsen Gao, Dechang Zeng, Lang Chen, Jun-Ming Liu, Albina Y. Borisevich, Jeffrey Bokor, Ramamoorthy Ramesh

Dr. D.Y. Chen, Prof. X.S. Gao
Institute for Advanced Materials and Guangdong Provincial Key Laboratory of Quantum Engineering and Quantum Materials
South China Normal University
Guangzhou 510006, China

Dr. D.Y. Chen, Dr. Z.H. Chen, Dr. C. R. Serrao, Dr. J. D. Clarkson, Prof. R. Ramesh
Department of Materials Science and Engineering
University of California, Berkeley
California, 94720, USA

Dr. D.Y. Chen, Prof. D.C. Zeng
School of Materials Science and Engineering
South China University of Technology
Guangzhou 510640, China

Dr. Q. He, Dr. A.Y. Borisevich
Materials Science and Technology Division
Oak Ridge National Laboratory
Oak Ridge, TN 37831, USA

Prof. L. Chen
Department of Physics
South University of Science and Technology of China
Shenzhen 518055, China

Prof. J.-M. Liu
Laboratory of Solid State Microstructures and Innovation Center of Advanced Microstructures
Nanjing University
Nanjing 210093, China

Dr. M. E. Nowakowski, Prof. J. Bokor, Prof. R. Ramesh
Department of Physics
University of California, Berkeley
California, 94720, USA

Keywords: BiFeO₃, multiferroic, depolarization field, domain wall, exchange bias

The atomic-scale growth techniques of oxide heterostructures provide a wealth of splendid possibilities for creating novel states at their interfaces, leading to a large number of emergent physical phenomena and functionalities as a consequence of the complex interplay of spin,

charge, orbital and lattice degrees of freedom. In ferroelectric materials, interfaces play a pivotal role in the formation of various domain structures, such as the observation of flux-closure polar domains in the ferroelectric/paraelectric $\text{PbTiO}_3/\text{SrTiO}_3$ multilayer films. Moreover, our recent study demonstrated that, due to the interplay between strain, depolarization field and gradient energies, topological ferroelectric vortices can be produced in $\text{PbTiO}_3/\text{SrTiO}_3$ superlattices. Interestingly, the domain structures can be engineered from a_1/a_2 domains to vortex–antivortex structures and then to classical flux-closure domain structures with the increase of the superlattice period, strongly depending on the interface effects of the depolarization field. Besides, extensive efforts have recently been focused on the control of domain structures through the tuning of depolarization field in PbTiO_3 , BaTiO_3 and $\text{Pb}(\text{Zr},\text{Ti})\text{O}_3$ thin films. By inserting a dielectric SrTiO_3 layer under the ferroelectric layer, Lichtensteiger et al. and Liu et al. showed that the domain configuration evolved from monodomain to polydomain as the thickness of SrTiO_3 space layer increases, in PbTiO_3 and $\text{Pb}(\text{Zr},\text{Ti})\text{O}_3$, respectively. Based on the prior work, here we are motivated to explore the interface engineering of domain structure evolution in BiFeO_3 (BFO) thin films by introducing a dielectric layer.

BFO is a room temperature multiferroic (ferroelectric and antiferromagnetic) with rhombohedral structure, giving rise to three possible domain patterns including 71° , 109° and 180° types. A large number of fascinating phenomena and functionalities have been discovered at the domain walls in BFO thin films, examples such as domain wall conductivity, photovoltaic effects, magnetoelectric coupling, enhanced magnetism and magnetotransport properties, enabling a wide variety of potential device applications for electronics, photonics and spintronics. Therefore, the ability to precisely control the domain structures (especially for the periodic domain structures) in BFO thin films is critical to enable the study of these exotic properties and the design of next generation of novel devices based on the domain wall functionalities.

Periodic ordered 71° , 109° and 180° stripe domains have been obtained through tuning of the electrostatic boundary conditions. Chu et al. showed that periodic 109° stripe domains can be produced in BFO thin films without or with very thin ($< 5\text{nm}$) SrRuO₃ (SRO) bottom electrode layer, while periodic 71° domain structures would form on thicker SRO ($> 25\text{nm}$), due to the screening effects from metal (SRO) -ferroelectric (BFO) interfaces. It has been shown that the exchange coupling between the ferromagnetic layer and multiferroic BFO layer enables an exchange enhancement of the ferromagnet with BFO 71° domain walls or both an exchange enhancement and exchange bias of the ferromagnet with 109° walls, providing the possibility of controlling ferromagnetism with an electric field, which has exciting application potentials in the low-energy-consumption, non-volatile magnetoelectronic memory devices. Indeed, the precise control of periodic 71° stripe domains on thick SRO bottom electrode (these domains are easy to switch by electric field) has promoted several seminal works on electric field control of magnetism in the ferromagnet /multiferroic BFO system. However, the periodic 109° stripe domains can only exist without (or with ultra-thin) SRO bottom electrode (these domains are very hard to switch or not switchable), inhibiting not only the study of switching behavior of 109° domains, but the potential to control the exchange bias using an electric field.

In this work, we demonstrate a depolarization field induced domain structure evolution in BiFeO₃ / LBFO (BFO/LBFO) multilayers and extend this discovery to BFO/LBFO superlattices. La_{0.25}Bi_{0.75}FeO₃ (LBFO), unlike the pure BFO with ferroelectric rhombohedral phase, possesses an equilibrium non-ferroelectric orthorhombic structure. we introduce LBFO as a dielectric layer between the bottom electrode (SRO) and the ferroelectric BFO layer to investigate the interface effects of depolarization field driven domain structure evolution. We show that periodic 71° stripe domains can be obtained in BFO film on DyScO₃ (DSO) substrate with SRO as the bottom electrode. In the BFO/LBFO/SRO multilayer heterostructures, the depolarization field induced by the LBFO (with thickness of $1 \sim 10\text{ nm}$)

layer can gradually drive 71° stripe domains to mixed 71° and 109° domains and then to pure periodic 109° stripe domains, which has also been confirmed in the BFO/LBFO superlattices with increasing the superlattice period. Furthermore, we demonstrate the origin of exchange bias in the $\text{Co}_{0.9}\text{Fe}_{0.1}(\text{CoFe})/\text{BFO}$ system through the magnetic interaction study between CoFe and BFO films with the pure 71° domain walls and pure 109° domain walls, respectively. The periodic 109° stripe domains with thick SRO bottom electrode also enable us to study its switching behavior and the possibility to realize electric field control of exchange bias at room temperature.

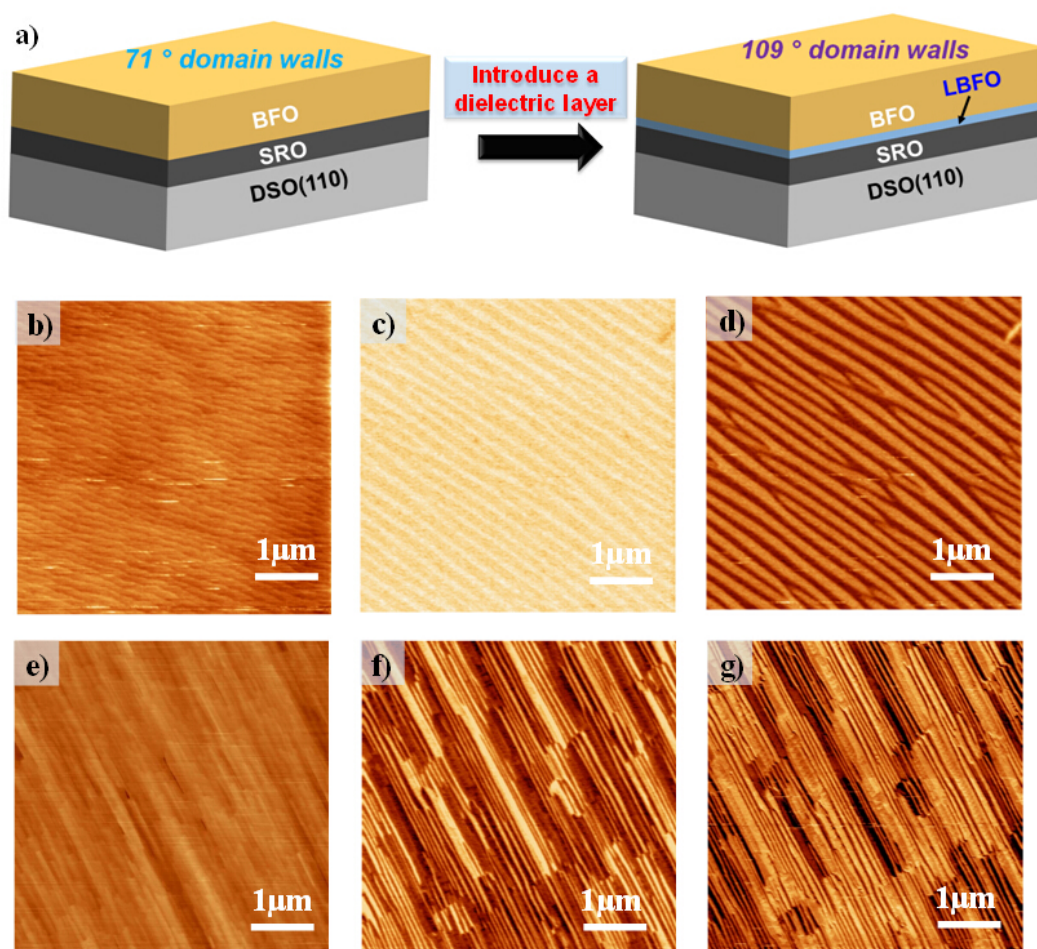


Figure 1. Domain “switch” by inserting a dielectric layer

We grew a series of epitaxial 100 nm-thick BFO films, without or with 1~10 nm dielectric LBFO layer on DSO(110) substrates with 30 nm SRO as the bottom electrode by pulsed laser deposition. The heterostructure stacks are displayed as the schematics in **Figure 1a**. Here, the domain structure evolution from 71° domains to 109° domains by introducing a dielectric

layer is predicted based on previous studies. A combination of piezoresponse force microscopy (PFM) and transmission electron microscopy (TEM) was used for the structure and ferroelectricity characterization. Magnetic properties were measured using superconducting quantum interference device (SQUID) and magneto-optic Kerr effect (MOKE).

The topography of the BFO/SRO/DSO sample is obtained by atomic force microscope (AFM) and is shown in Figure 1b. The atomically flat terraces with one unit cell in height confirm the high quality coherent growth of the film, with the root mean square (RMS) roughness only 0.2 nm. The uniform contrast of the out-of-plane PFM image (Figure 1c) and the stripe-like contrast of the in-plane image (Figure 1d) confirm the formation of periodic 71° stripe domains in BFO/SRO/DSO, which is consistent with previous work by Chu et al. Then, we introduced a thin layer (~ 10 nm) of LBFO between BFO and SRO, i.e., the multilayer BFO/ LBFO /SRO/DSO was established. The topography (Figure 1e) also suggests the high quality of the film. Interestingly, the periodic 71° stripe domains, as shown in Figure 1c and 1d, are “switched” to periodic 109° domains (Figure 1f, g), which show stripe-like contrast both out-of-plane (Figure 1f) and in-plane (Figure 1g) PFM images, by inserting the LBFO layer. The key question arising here is to explore the “switching” mechanism of this phenomenon. Previous work has demonstrated that the SrTiO_3 dielectric layer can be used to increase the depolarization field and hence induce the monodomain to polydomain evolution in PbTiO_3 and $\text{Pb}(\text{Zr},\text{Ti})\text{O}_3$. Here, we first time report a dielectric layer can be introduced to drive the periodic 71° stripe domains to 109° stripe domains in BFO films. We infer that the depolarization field arising from the LBFO layer plays a key role in the domain structure evolution from 71° stripe domain to periodic 109° domain in BFO.

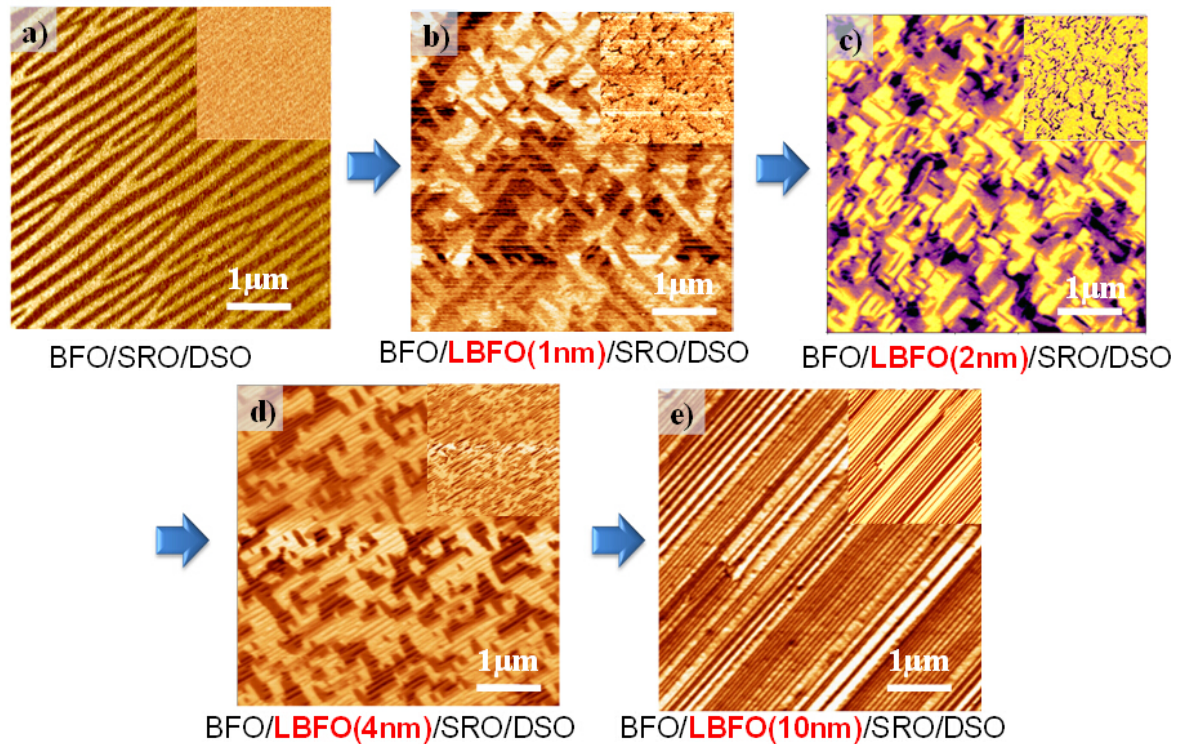


Figure 2. Domain structure evolution with the increasing thickness of LBFO layer

To further understand how the LBFO layer affects the formation of domain structures in the BFO layer, a series of LBFO films with various thickness (0~10 nm) were grown between the BFO layer (~100 nm) and SRO (~30 nm) layer on DSO (110) substrate, stacking as BFO/LBFO /SRO /DSO multilayer heterostructures. Using PFM, we investigate the domain configuration of BFO in these heterostructures, focusing on the effect of the LBFO thickness in the domain structure evolution, which are displayed in **Figure 2**. Detailed analyses, combining of both in-plane (Figure 2a-e) and out-of-plane (insets in the top-right of Figure 2a-e) PFM images of the samples with different thickness (0~10nm) LBFO layer, enable us to identify the types of ferroelectric domain walls. Here, as shown in Figure 2a-e, all the in-plane PFM images show stripe-like contrast, thus the uniform out-of-plane contrast presents the pure 71° domain walls while the existence of black contrast in the out-of-plane images imply the presence of 109° domain walls. It is revealed that pure 71° stripe domains without LBFO layer (Figure 2a) gradually evolve to mixed 71° and 109° domain structures, where the fraction of 109° domains (which can be identified from the out-of-plane image contrast)

gradually increases with the increasing thickness of LBFO from 1 nm to 4 nm (Figure 2b-d), and finally turn into pure 109° stripe domain walls with 10 nm-thick LBFO (Figure 2e).

Based on the PFM data in Figure 1 and Figure 2, we can now better understand the role played by LBFO layer in controlling the domain structures in the BFO layer. In the BFO/SRO/DSO stack (without LBFO), the screening effects at the ferroelectric(BFO)/metal(SRO) interface enable the formation of 71° domains, while the introduce of the LBFO dielectric space layer increases the distance between the screening charges from the bottom electrode SRO and ferroelectric BFO polarization, reducing the screening effects and hence increasing the depolarization field. Consequently, the 71° stripe domain is destabilized and 109° stripe domain structure forms to reduce the energy cost owing to this strong depolarization field. Therefore, through changing the thickness of the LBFO layer, the depolarization field can be manipulated to design and control the domain configuration of BFO film.

The ability to accurately control the 71° and 109° stripe domains, demonstrated in this letter, enables us to study the switching behavior of these domain structures, which is essential for exploiting the domain wall functionality and magnetoelectric device applications. It is worth to note that we are able to study the switching behavior of the BFO 109° stripe domains for the first time due to the presence of SRO bottom electrode. **Figure 3** shows the topography, out-of-plane and in-plane PFM images of the samples after applying the direct current (DC) electric field. $5\ \mu\text{m} \times 5\ \mu\text{m}$ PFM images of all the samples were taken after poling $3\ \mu\text{m} \times 3\ \mu\text{m}$ boxes with a minus DC field and the poling $1\ \mu\text{m} \times 1\ \mu\text{m}$ boxes with a corresponding positive DC field. Distinct switching behaviors are observed in the films with different domain structures. As shown in Figure 3a-c, it is revealed that periodic 71° stripe domains in the BFO/SRO/DSO heterostructure can be switched back and forth after the -6 V and 6 V DC field poling, which is in agreement with earlier study. The reversible switching of

71° domains has stimulated the study of electric field control of magnetism in the ferromagnet/multiferroic BFO heterostructures.

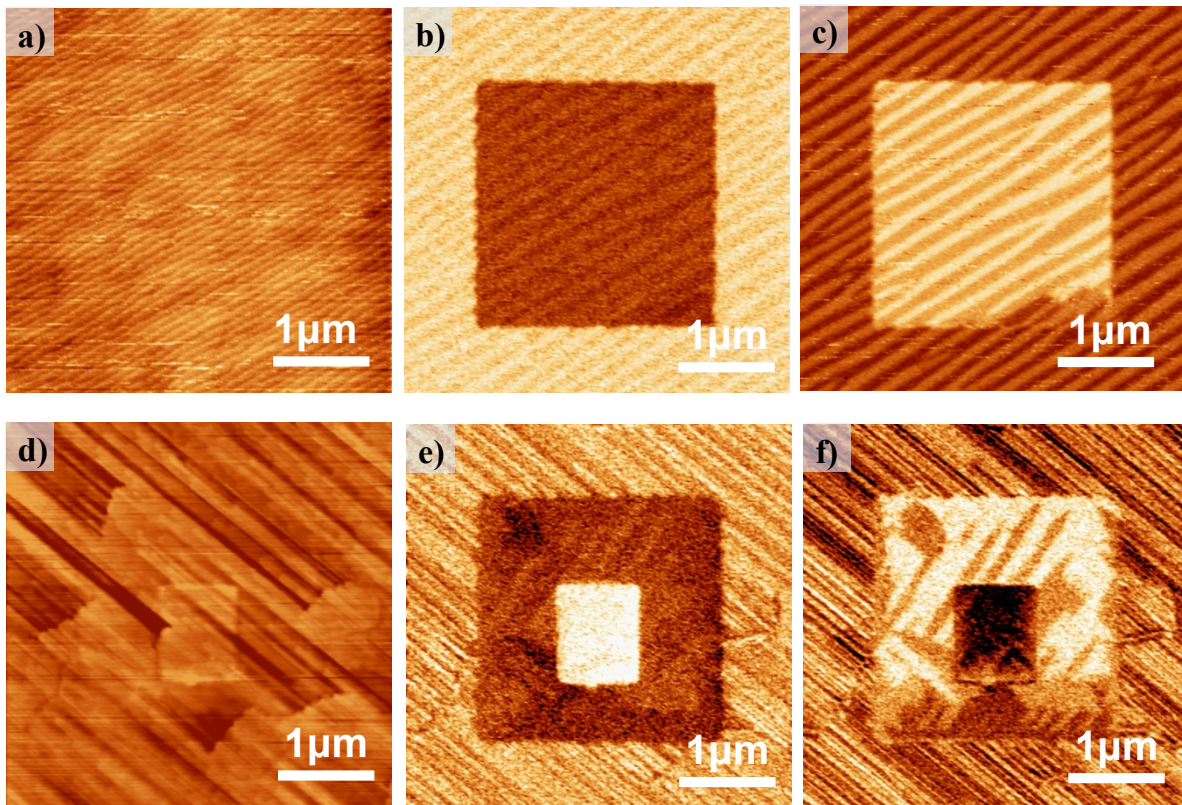


Figure 3. Switching behavior of 71° and 109° domain structures

Recently, strong exchange bias has been reported in the ferromagnet/multiferroic BFO system with 109° domain walls, opening a new possibility to realize the electric field control of exchange bias. However, Allibe *et al.* reported that the exchange bias can not be reversibly manipulated by electric field in a CoFeB/ BFO (with mosaic domains including 71° and 109° domains) based spin valve. The switching behavior study of 109° stripe domains may help to understand the reason why the exchange bias is not reversibly switched using electric field. According to the out-of-plane and in-plane PFM images in Figure 3d-f, we find that the periodic 109° stripe domains are predominately switched to 71° or single domain after applying -6 V and 6 V DC field. Therefore, the 109° stripe domains can not be switch back and forth, leading to the decline of exchange bias in the previous study. Detailed study of the switching behavior of 109° domain with the increasing poling DC field from 1V to 9V is

shown in Figure S1. It further confirms that, by applying a DC voltage on the film, we can effectively “erase” areas of 109° domain walls. These switching events result in 71° domain walls or single domain state. The important topic of how to switch 109° stripe domains back and forth is still under further study in our group, which is critical for the study of electric field control of exchange bias.

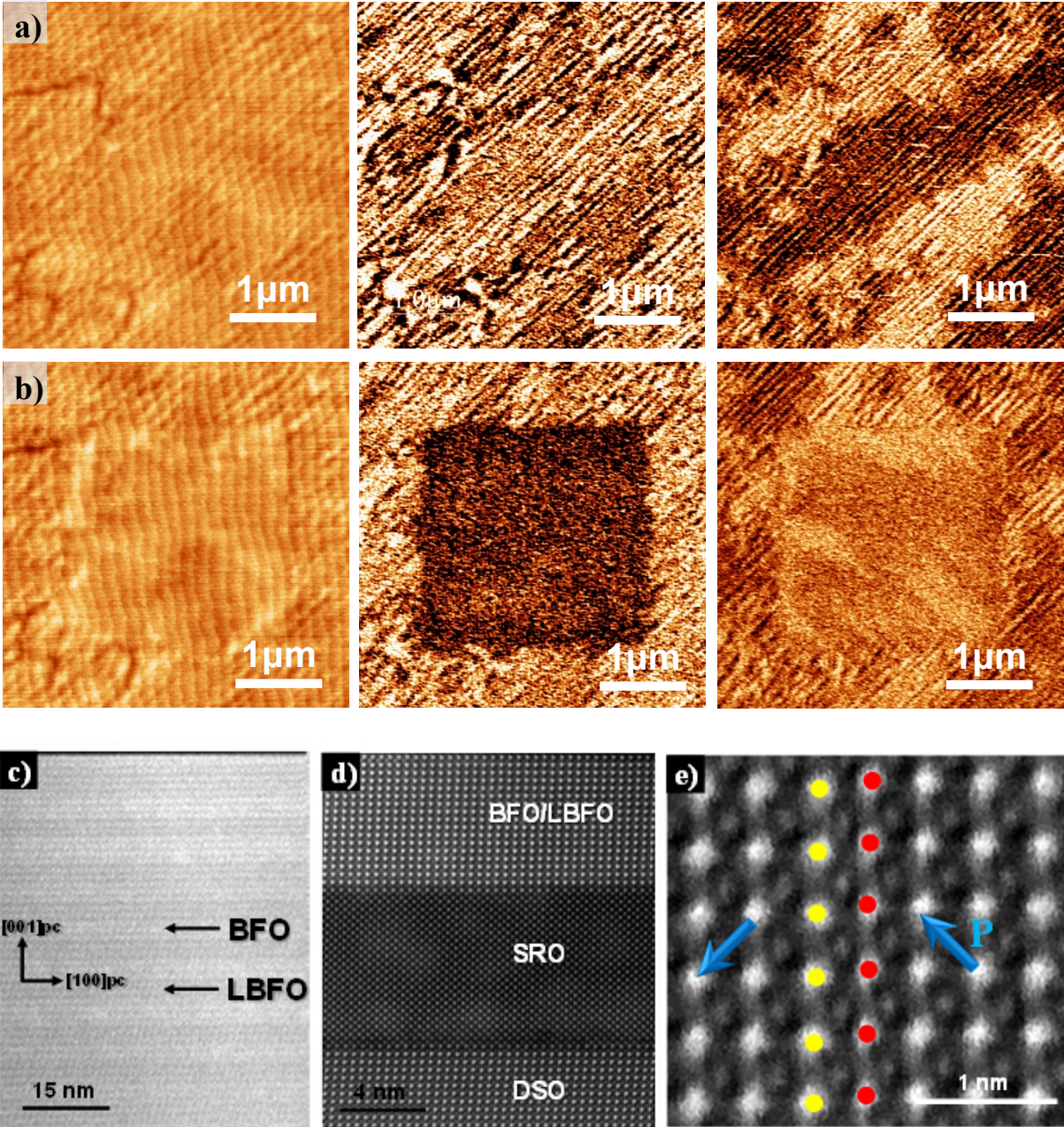


Figure 4. Periodic 109° domain patterns in 10×10 BFO/LBFO superlattices
 After successfully realizing the depolarization field driven domain structure evolution in BFO films, we next try to extend this interface engineering effect to BFO/LBFO superlattices.

Symmetric (BFO) n /(LBFO) n superlattices with $n = 3, 10, 20$ were synthesized on DSO (110) substrates via pulsed-laser deposition. Here, superlattices are referred to using the ' $n \times n$ ' shorthand wherein n corresponds to the thickness of the BFO and LBFO layers in unit cells. As shown in Figure S2, **Figure 4a,b** and Figure S3, the topography, out-of-plane and in-plane PFM images of the 3×3 , 10×10 and 20×20 BFO/LBFO samples are shown from left to right. It is found that the PFM images of 3×3 (Figure S2a) BFO/LBFO superlattices show mixed 71° and 109° domain structures, while 10×10 (Figure 4a) and 20×20 (Figure S3a) superlattices possess periodic 109° stripe domains, implying the interface engineering of domain structure evolution in the BFO/LBFO superlattices with increasing superlattice period, as thicker LBFO layer can produce larger depolarization field. The switching behaviors of these superlattices are also studied (displayed in Figure S2b, Figure 4b and Figure S3b), it further confirms that the 109° domains are switched to 71° domains or single domain.

A cross sectional image of the BFO/LBFO superlattices is shown in Figure 4c taken by high-angle annular dark field (HAADF) scanning-TEM (STEM). The image shows that the BFO/LBFO superlattices have high quality epitaxial growth, revealing the layer uniformity with sharp BFO/LBFO interfaces. This type of image is sensitive to variations in atomic number (Z number), and the composition changes between the layers of the heterostructure are clearly distinguished. The intensity corresponds to increasing Z number, so the elements in decreasing order of brightness are Bi(83)/La(57), Sr(38), Fe(26), Ti(22), and O (8) is too light to be visible. A high-resolution Z -contrast image of the SRO/DSO and BFO/SRO interfaces is shown in Figure 4d, illustrating the atomic-scale epitaxy between the SRO and DSO substrate and (La)BFO/SRO layers. As shown in Figure 4c, the bright layers are BFO layer and the dark ones are LBFO because Bi(83) is heavier than La(57), and the sharp BFO/LBFO interface can be identified. However, the interface of BFO/LBFO can not be identified in this high-resolution STEM image (Figure 4d) because the compositions of the two layers are not sufficiently distinguished. The HAADF STEM image displayed in Figure

4e and the dark field cross-sectional TEM image shown in Figure S4 further confirm that the 109° domain walls are obtained in BFO/LBFO superlattices, which is consistent with the PFM data in Figure 4a.

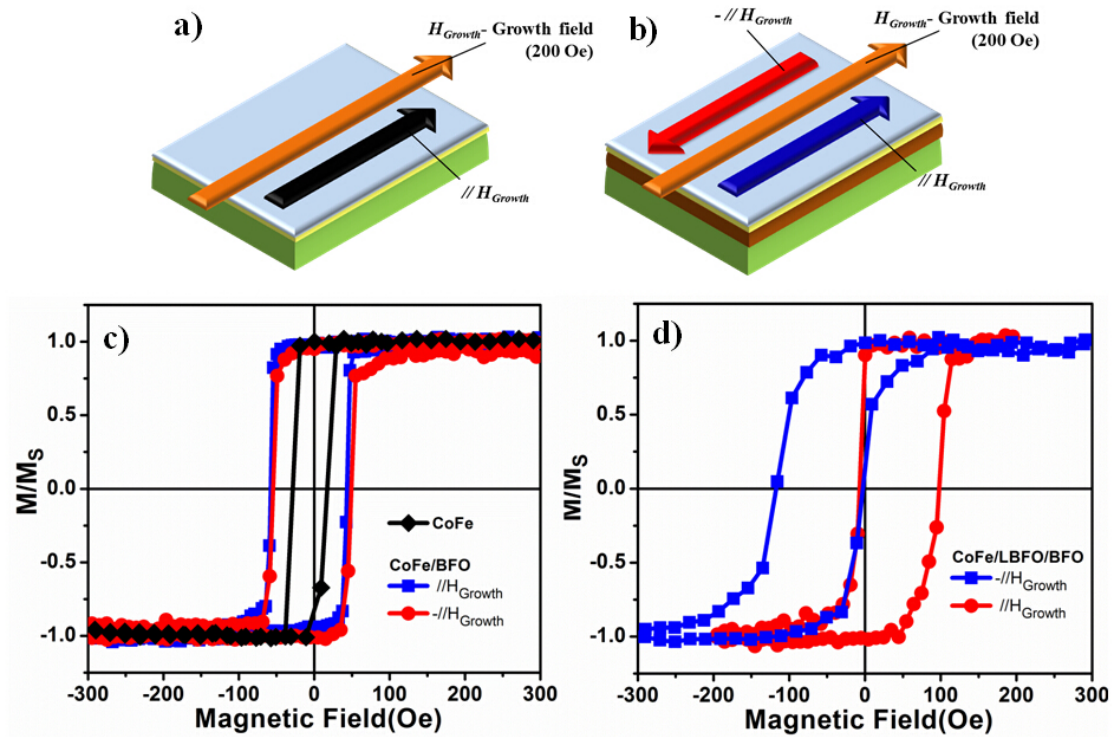


Figure 5. Exchange coupling in CoFe/BFO (71° domain wall) and CoFe/LBFO/BFO (109° domain wall) structures.

We next turn to the study of magnetic interactions in the CoFe/BFO heterostructures. CoFe (2.5 nm) and Pt (2.5 nm) layers were deposited on BFO/SRO/DSO sample (with pure periodic 71° domain walls) and BFO/LBFO/SRO/DSO stack (with pure periodic 109° domain walls) via sputtering system, respectively. CoFe and Pt were also deposited directly to the DSO substrates to compare the behavior of the Pt/CoFe/DSO stack to the Pt/CoFe/BFO/SRO/DSO and Pt/CoFe/BFO/LBFO/SRO/DSO stacks. The growth of the CoFe layer was completed in an applied magnetic field of 200 Oe (H_{Growth}) to induce unidirectional anisotropy in the CoFe/BFO heterostructures. **Figure 5a,b** provide a schematic illustration to explain the orientation of applied magnetic growth field and the direction of the

magnetic field during the SQUID measurement. It is important to note that two distinctly different types of behavior are found. In Figure 5c, SQUID measurement parallel to H_{Growth} shows very small H_c ($\sim 10-15$ Oe) with almost no shift of the M-H loop in the Pt/CoFe/DSO stack. Only the exchange enhancement ($H_C \sim 50$ Oe) is observed (Figure 5c) in the CoFe/BFO system with 71° domain walls, while the CoFe/BFO/LBFO sample with 109° domain walls, as shown in Figure 5d, exhibits both a strong exchange bias (typical $|H_{EB}| \sim 50$ Oe) and significant enhancement of H_C ($H_C \sim 50$ Oe). Confirmation of such exchange bias interaction is obtained upon 180° rotation of the samples, where one can observe the opposite shift of the hysteresis loop when measured antiparallel to H_{Growth} (Figure 5d). The exchange bias in CoFe/BFO/LBFO has also been confirmed via MOKE measurement (Figure S5). In the BFO mosaic domain structures, previous study has demonstrated that 109° domain walls can play an important role in determining the exchange bias in CoFe/BFO system. Here, the precise controlling of pure 71° and 109° periodic stripe domain walls enable us to make a clear demonstration that the exchange bias in the CoFe/BFO system originates from the pinned, uncompensated 109° domain walls in BFO.

In summary, our studies have revealed the ability to precisely control the domain structure evolution by tuning the depolarization field with a dielectric layer in multilayer BFO/LBFO/SRO/DSO heterostructures. This interface effect has also been successfully extended to the BFO/LBFO superlattices. Furthermore, the 109° stripe domain structures with SRO bottom electrode enable us to study the switching behavior for the first time. We also report a clear demonstration of the origin of exchange bias in CoFe/BFO system is from the 109° domain walls. These findings provide the future direction to study electric field control of exchange bias and open a new pathway to explore the room temperature multiferroic vortices in multiferroic BFO system such as BFO/LBFO superlattices.

Experimental Section ((delete section if not applicable))

Experimental Subheading: Experimental Details. 12 point, double-spaced. References are superscripted and appear after the punctuation.^[6]

Supporting Information

Supporting Information is available online from the Wiley Online Library or from the author.

Acknowledgements

((Acknowledgements, general annotations, funding.))

Received: ((will be filled in by the editorial staff))

Revised: ((will be filled in by the editorial staff))

Published online: ((will be filled in by the editorial staff))

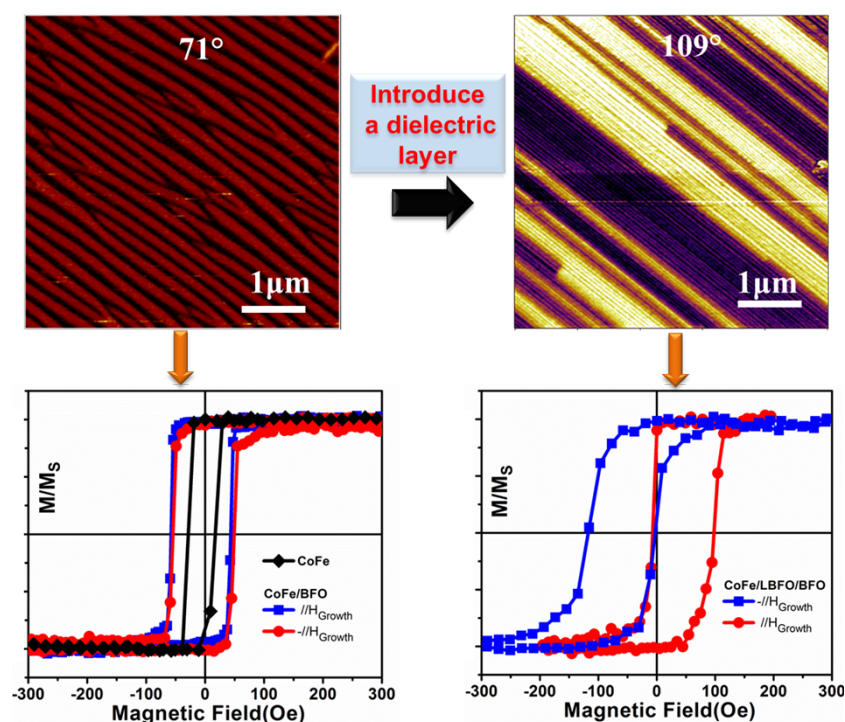
The depolarization field driven domain structure evolution has been demonstrated by inducing a dielectric layer, both in $\text{BiFeO}_3/\text{La}_{0.25}\text{Bi}_{0.75}\text{FeO}_3$ (BFO/LBFO) multilayers and BFO/LBFO superlattices. This interface effect enables the formation of periodic stripe 109° domains with bottom electrode to study its switching behavior and reveal the origin of the exchange bias in the ferromagnet/BFO system.

Keyword: BiFeO_3 , multiferroic, depolarization field, domain wall, exchange bias

Deyang Chen, Zuhuang Chen, Qian He, Claudy R. Serrao, James D. Clarkson, Ajay Yadav, Mark E. Nowakowski, Xingsen Gao, Dechang Zeng, Lang Chen, Jun-Ming Liu, Albina Y. Borisevich, Jeffrey Bokor, Ramamoorthy Ramesh

Interface engineering of domain structures in BiFeO_3 thin films

ToC figure ((Please choose one size: 55 mm broad \times 50 mm high or 110 mm broad \times 20 mm high. Please do not use any other dimensions))



Copyright WILEY-VCH Verlag GmbH & Co. KGaA, 69469 Weinheim, Germany, 2013.

Supporting Information

for *Adv. Mater.*, DOI: 10.1002/adma.((please add manuscript number))

Interface engineering of domain structures in BiFeO₃ thin films

Deyang Chen, Zuhuang Chen, Qian He, Claudy R. Serrao, James D. Clarkson, Ajay Yadav, Mark E. Nowakowski, Xingsen Gao, Dechang Zeng, Lang Chen, Jun-Ming Liu, Albina Y. Borisevich, Jeffrey Bokor, Ramamoorthy Ramesh

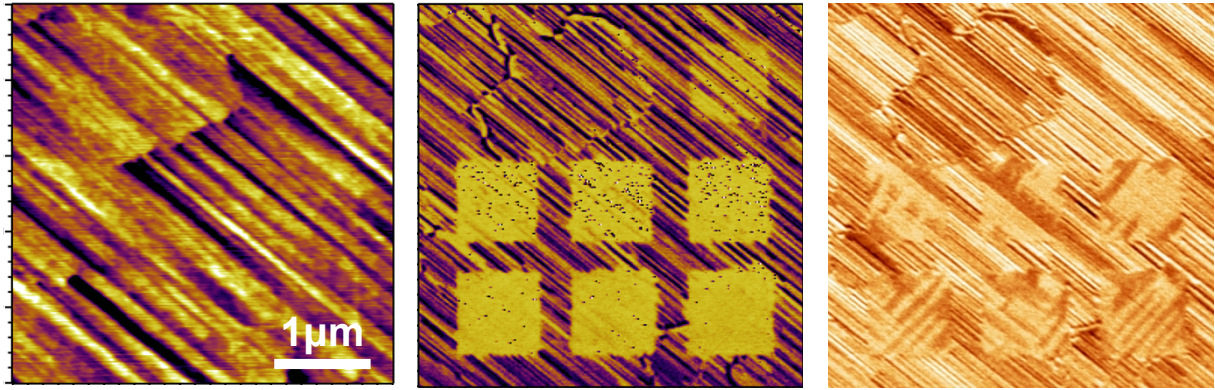


Figure S1. Switching behavior of 109° domains with the applied DC field from 1V to 9V.

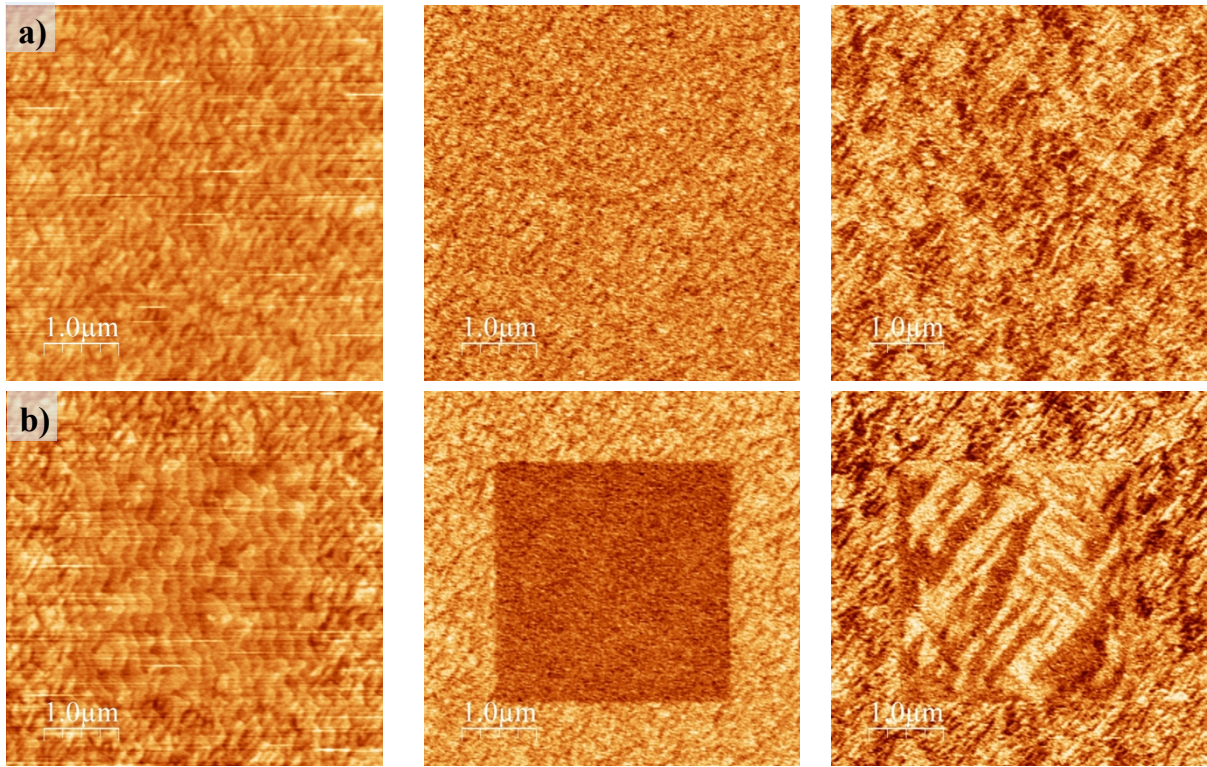


Figure S2. mixed 71° and 109° domain walls in 3×3 LBFO/BFO superlattices

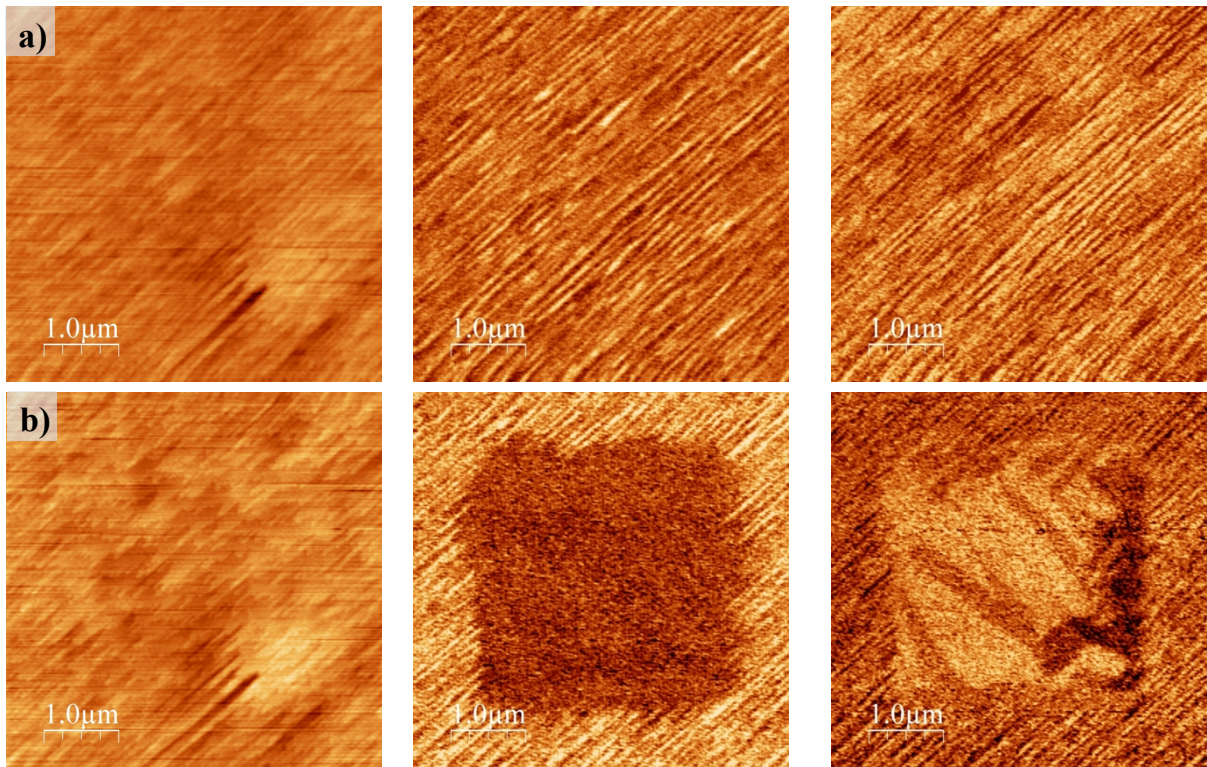


Figure S3. periodic 109° domain walls in 20×20 LBFO/BFO superlattices

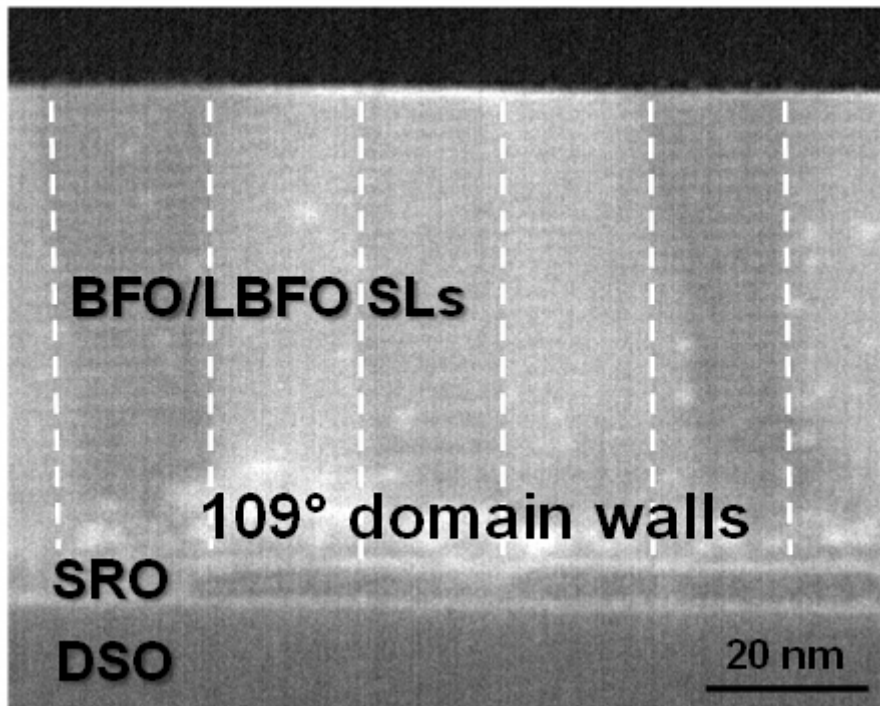


Figure S4. Dark field cross-sectional TEM image of LBFO/BFO superlattices shows the 109° domain walls.

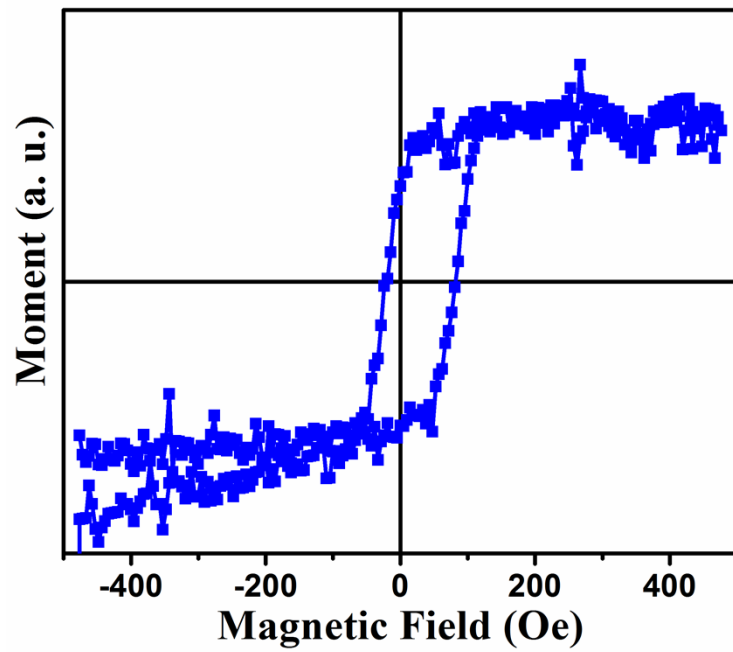


Figure S5. MOKE measurement of the exchange bias in Pt/CoFe/BFO/LBFO/SRO/DSO structures with 109° domain walls